

PAPER • OPEN ACCESS

## Iron(II) complexes with $N_2O_2$ coordinating Schiff base-like equatorial ligand and 1,2-bis(pyridin-2-ylethynyl)benzene as axial pincer ligand

To cite this article: Sophie Schönfeld *et al* 2019 *J. Phys.: Condens. Matter* **31** 504002

View the [article online](#) for updates and enhancements.

You may also like

- [Spectral and cyclic voltammetry studies of chloro-salicyliden aniline and some of its complexes with Co\(II\) and Mn\(II\)](#)  
Salih Hamza Abbas, Diyar Mohammad Ali Murad and Hayat Hamza Abbas
- [Coordination compounds of biogenic metals as cytotoxic agents in cancer therapy](#)  
Dmitry A. Guk, Olga O. Krasnovskaya and Elena K. Beloglazkina
- [The electric and thermoelectric properties of Cu\(II\)-Schiff base nano-complexes](#)  
E M M Ibrahim, Laila H Abdel-Rahman, Ahmed M Abu-Dief et al.

# Iron(II) complexes with N<sub>2</sub>O<sub>2</sub> coordinating Schiff base-like equatorial ligand and 1,2-bis(pyridin-2-ylethynyl)benzene as axial pincer ligand

Sophie Schönfeld<sup>1</sup>, Charles Lochenie<sup>2</sup>, Gerald Hörner<sup>1</sup>  and Birgit Weber<sup>1,3</sup> 

<sup>1</sup> Department Chemie, Universität Bayreuth, Bayreuth, Germany

<sup>2</sup> Institut de Science et d'Ingénierie Supramoléculaires (ISIS), Université de Strasbourg, Strasbourg, France

E-mail: [weber@uni-bayreuth.de](mailto:weber@uni-bayreuth.de)

Received 24 May 2019, revised 23 July 2019

Accepted for publication 27 August 2019

Published 20 September 2019



## Abstract

Three new unique mononuclear iron(II) pincer complexes were synthesized using 1,2-bis(pyridin-2-ylethynyl)benzene as axially coordinating pincer ligand and N<sub>2</sub>O<sub>2</sub> coordinating Schiff base-like equatorial ligands. Magnetic susceptibility measurements reveal that all three complexes remain in the high spin state throughout the entire temperature range investigated. Reasons for this are restraining sterical interactions revealed in the single crystal x-ray structure analysis and extended DFT-computational studies of one of the pincer complexes. Those interactions also lead to the formation of unexpected side products during the synthesis such as a complex with two ethanol molecules as axial ligand, whose x-ray structure was determined.

Keywords: iron complex, pincer ligand, Schiff base ligand, magnetism

 Supplementary material for this article is available [online](#)

(Some figures may appear in colour only in the online journal)

## 1. Introduction

An extensively and very interdisciplinary studied field in coordination chemistry are iron(II) spin-crossover (SCO) complexes. In those molecules the spin state can be reversibly switched between the paramagnetic high spin (HS) and the diamagnetic low spin (LS) state owing to external stimuli such as temperature change, pressure change or light irradiation [1]. An especially intriguing aspect of those compounds is that the switching behaviour is a molecular property. Thus, in theory at least, it is possible to switch each molecule independently—an

highly interesting aspect for the development of molecular electronics and spintronics [2]. By this way, information could be stored in a single molecule enabling high storage densities. Investigations on such materials require the deposition of the single molecules on a surface, thus robust and usually charge neutral spin crossover complexes are required with a sufficiently high complex stability [3]. This precondition is fulfilled by complexes with multidentate ligands [4].

Tetra-dentate N<sub>2</sub>O<sub>2</sub> coordinating Schiff base-like ligands were shown to be highly suitable for the synthesis of iron(II) spin crossover complexes if combined with pyridine-based axial ligands [5–8]. The original ligand system, first reported by Jäger *et al.* [8], is very flexible with regard to modifications to achieve multifunctionality (e.g. luminescence [9], magnetic exchange interactions [10], softness [11, 12]), while maintaining the spin crossover properties. So far, however,

<sup>3</sup> Author to whom all correspondence should be addressed.

 Original content from this work may be used under the terms of the [Creative Commons Attribution 3.0 licence](#). Any further distribution of this work must maintain attribution to the author(s) and the title of the work, journal citation and DOI.

the corresponding mononuclear complexes lack the stability necessary for deposition on a surface since two monodentate axial ligands are used to reach the octahedral coordination sphere necessary for the observation of spin crossover [13]. In order to obtain both spin-crossover behaviour and the stability of coordination compounds with multidentate ligands, in this study we aim to use 1,2-bis(pyridin-2-ylethynyl)benzene (bpeb) as axially trans-coordinating pincer ligand. This would lead to the formation of a heteroleptic octahedral complex molecule with two chelate ligands of different nature. Such complexes are highly interesting as they would allow different functionalization on the two different ligand sides. Recently, several interesting iron(II) and iron(III) spin crossover complexes were reported using different bidentate or tridentate ligands [14]. Here we use a tetradentate ligand in combination with a bidentate pincer ligand. Pincer complexes are known to be sturdy and in case of catalytic activity also highly selective [15]. Bosch and Barnes first reported bpeb as a novel trans-chelating bipyridyl ligand that complexes silver and palladium [16]. A variety of mono- and oligonuclear bpeb complexes with palladium and silver [16, 17], copper, cobalt and rhodium [18] and even mercury [19] as the central ion are reported by now. With the best of our knowledge, there is still no bpeb containing complex with iron as the central ion reported. If one compares the bond lengths between the metal centre and the coordinating nitrogen atoms presented in these works, it becomes clear that the ligand is flexible in a range of 1.91–2.63 Å. In iron (II) SCO complexes, the SCO also involves a change in bond length (about 2.01 Å (Fe–N<sub>ax</sub>) in the LS state and about 2.24 Å (Fe–N<sub>ax</sub>) in the HS state).[8] It is therefore to be examined whether the flexibility of the ligand bpeb has a positive effect on spin-transition behaviour of iron (II) complexes, thus facilitating an SCO.

## 2. Results and discussion

The synthesis of the pincer-ligand bpeb was carried out as described in the literature [16, 17]. For the synthesis of the octahedral pincer-complexes a one-pot reaction was used with the related mononuclear iron(II) complexes with methanol as axial ligands as starting material [6, 20]. As initial attempts with methanol as solvent were not successful in all cases, ethanol and acetonitrile were also used as solvents for the ligand substitution reaction with the pincer-ligand. An overview of the different products is given in table 1. In scheme 1 the general synthesis pathway for the desired complexes is given.

While usually ethanol or methanol are well suited to obtain the desired octahedral complexes [8], in the case of [FeL1c] only the starting material was obtained. For this complex, CH<sub>3</sub>CN proved to be a suitable solvent for the isolation of the desired product. With the adopted reaction conditions, the complexes [FeL1a(bpeb)] (1), [FeL1b(bpeb)] · (EtOH) (2) and [FeL1c(bpeb)] (3) were obtained in good yields. The complexes were fully characterized by elemental analysis, IR spectroscopy, mass spectrometry and Mössbauer spectroscopy. There was no mass peak detected of the intact pincer complex during mass spectrometry. However the equatorial ligand and the pincer ligand bpeb could be found as separate

**Table 1.** Overview of the used synthesis conditions and the obtained products. Ligand:[FeL1x(MeOH)<sub>2</sub>] ratio = 2:1.

Ligand	Solvent	Product	yield [%]
L1a	MeOH	[FeL1a(bpeb)] (1)	48
L1b	EtOH	[FeL1b(bpeb)] · (EtOH) (2)	48
L1c	MeOH	[FeL1c(MeOH) <sub>2</sub> ]	20
	EtOH	[FeL1c(EtOH) <sub>2</sub> ]	28
	MeCN	[FeL1c(bpeb)] (3)	59

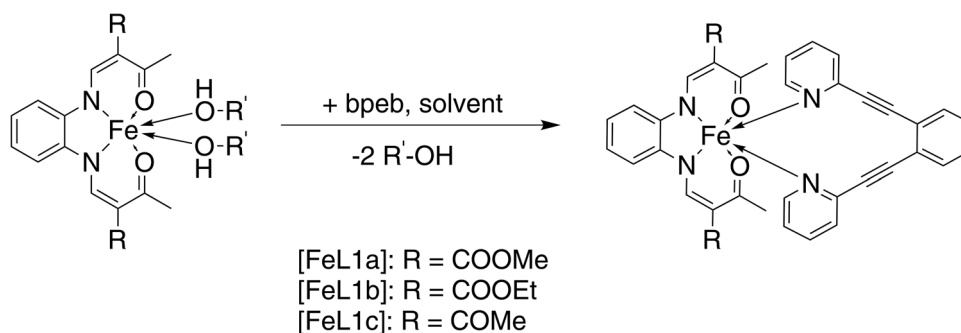
peaks. The harsh conditions of the DEI+ measurement obviously cause the pincer to dissociate. Softer measurement methods are required to detect the intact complex. Crystal structures were obtained via x-ray diffraction analysis of single crystals for 3 and for the side product [FeL1b(EtOH)<sub>2</sub>] (4) and will be discussed in the following.

### 2.1. X-ray structure analysis

Single crystals suitable for x-ray structure analysis were either obtained from the filtrate of 2 leading to the ethanol complex 4 or straight from the reaction mixture after cooling down to room temperature for 3. The crystallographic data of the two complexes were collected at 133 K and are summarized in table S1 (available online at [stacks.iop.org/JPhysCM/31/504002/mmedia](http://stacks.iop.org/JPhysCM/31/504002/mmedia)).

Complex 3 crystallizes in the orthorhombic space group *Pbca* with eight formula units in the unit cell. Figure 1 displays the ORTEP drawing of the asymmetric unit together with the used atom numbering scheme. The octahedral N<sub>4</sub>O<sub>2</sub> coordination sphere of the iron(II) center consists of the Schiff base-like equatorial ligand and the axially coordinated pincer-ligand bpeb, bound through the terminal pyridyl groups. Selected bond lengths and angles within the inner coordination sphere are summarized in table 2.

The average bond lengths of 3 are 2.13 Å (Fe–N<sub>eq</sub>), 2.02 Å (Fe–O<sub>eq</sub>) and 2.27 Å (Fe–N<sub>ax</sub>) and are within the range reported for HS iron(II) complexes of this ligand type.[7, 8, 11, 21] The angle O<sub>eq</sub>–Fe–O<sub>eq</sub> is with 116.73(4)° in a region characteristic for the HS state, but appears quite large if compared to similar complexes.[7, 8] This could be attributed to steric aspects discussed in the following. The N<sub>ax</sub>–Fe–N<sub>ax</sub> angle is with 166.89(8)° strongly bent and not in a range typical for octahedral complexes of this general type [7, 8]. To determine the deformation of an octahedron the parameter  $\Sigma$  can be used.  $\Sigma$  refers to the deviations from 90° of all 12 cis angles within the inner coordination sphere. In table S2 (ESI) all corresponding angles are listed. For the discussed bpeb pincer ligand complex  $\Sigma$  differs with a value of 92.13 significantly from 0 what would be typical for an ideal octahedron.[25] The already published compound [FeL1c(py)<sub>2</sub>] has a quite similar coordination sphere.[26] With a value of  $\Sigma = 50.54$  this complex is also octahedral distorted but quite less than the pincer complex considered in this work. Examination of the bonds in the molecule reveals that the equatorial ligand is not planar but bent on one side. Supporting this statement table S3 (ESI) displays the dihedral angles of the asymmetric unit of 3.



**Scheme 1.** Ligand substitution reaction used for the synthesis of the iron(II) pincer-complexes 1–3 and used abbreviations.

The C(12)–O(2)–Fe(1)–O(1) angle ( $-134.7(2)^\circ$ ) differs significantly from the nominally equivalent dihedral angle between C(1)–O(1)–Fe(1)–O(2) ( $164.6(2)^\circ$ ). In line with this, the angle between the planes of the two six-chelate rings O1–C(1)–C(2)–C(3)–C(4)–N(1) and O(2)–C(12)–C(11)–C(10)–N(2) gives  $37^\circ$  what is large, indicating a strongly bent structure of the usually planar Schiff base-like ligand. This strong distortion is also reflected in the distances between the iron center and the axial bpeb nitrogens, which differ by 0.1 Å. The data indicates that the coordination of the bpeb ligand towards the metal centre is impeded. The distances between the coordinating oxygen atoms and the carbon atoms participating in the triple bond are with 2.99 Å (O(1)–C(24)) and 3.27 Å (O(2)–C(24)) quite short. Therefore it is most likely steric hindrance between the triple bonds of the bpeb ligand and the oxygen donor atoms of the Schiff base-like ligand causing the impediment. This leads to a bending of the equatorial ligand and may also explain the unexpected difficulties encountered during the synthesis. Figure 2 displays the packing pattern of 3 in the crystal. The pattern is dominated by  $\pi$ – $\pi$  interactions between the aromatic rings N(3)–C(19)–C(20)–C(21)–C(22)–C(23) and C(26)–C(27)–C(28)–C(29)–C(30)–C(31) of the pincer ligand.

In figure 3, those interaction occurring between the benzene ring of one bpeb molecule and the pyridine ring of a neighbouring bpeb molecule are illustrated in more detail. Selected distances (Å) and angles ( $^\circ$ ) of the  $\pi$ – $\pi$  interaction are summarized in table 3. There are no classical hydrogen bonds in the crystal packing, however, three characteristic short contacts (non-classical hydrogen bonds) that further support the packing of the molecules in the crystal are observed (pink dashed lines in figure 2), that are summarized in table 4.

The side product [FeL1b(EtOH)<sub>2</sub>] (4) crystallizes in the triclinic space group  $P\bar{1}$ , with two formula units in the unit cell. On the bottom of figure 4 the ORTEP drawing of the asymmetric unit together with the used atom numbering scheme is displayed. The octahedral coordination sphere of the iron(II) centre consists of the Schiff base-like equatorial ligand and two axially coordinated ethanol molecules. Selected bond lengths and angles within the inner coordination sphere are summarized in table 2. Both, bond lengths and angles, are in a range typical for HS iron(II) complexes of this general ligand type [7, 8, 11, 21].

The mean value of the  $O_{\text{eq}}\text{--Fe--}O_{\text{eq}}$  angle amounts to  $111.73(4)^\circ$  which is clearly in the range characteristic of

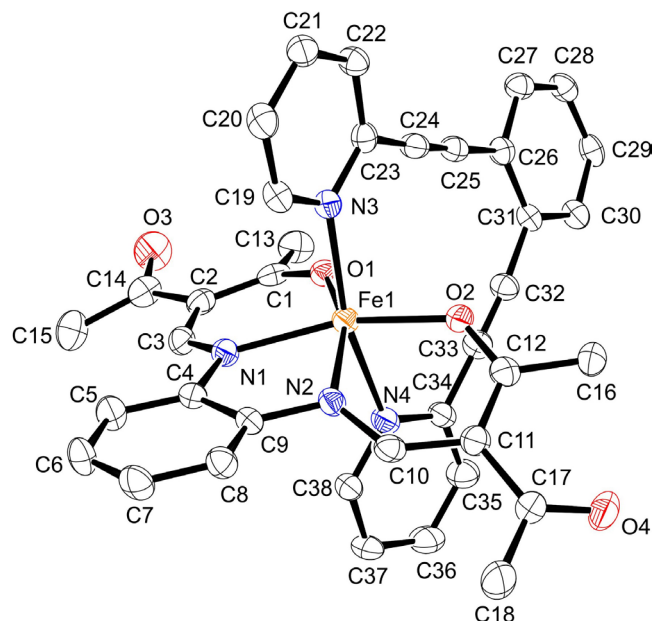


**Figure 1.** ORTEP drawing of the asymmetric unit of 3 with the atom-numbering scheme used in the text. Hydrogen atoms are omitted for clarity. Thermal ellipsoids presented at 50% level.

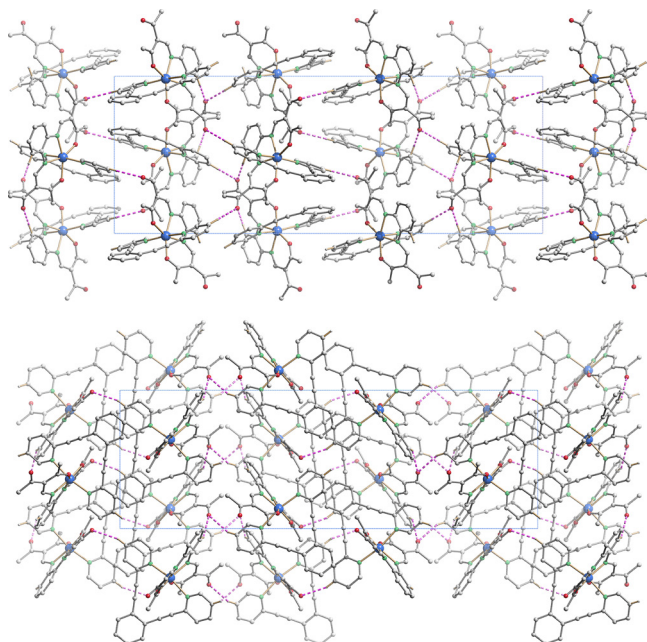
HS iron(II) complexes [8, 22, 23]. Please note that both, the average Fe–O<sub>ax</sub> bond lengths (2.20 Å) and the O<sub>eq</sub>–Fe–O<sub>eq</sub> angle, are smaller compared to the bpeb complex 3. The angle between the planes spanned by the two six-membered chelate rings of the Schiff base-like ligand of  $18^\circ$  is also significantly smaller.

If one considers the  $\Sigma$  value of 4 ( $\Sigma = 52.3$ ) it becomes clear that the complex is as well no ideal octahedron. But in comparison with the pincer complex the coordination centre is less distorted. In line with this, the O<sub>ax</sub>–Fe–O<sub>ax</sub> angle ( $169.4^\circ$ ) does also differ from the ideal  $180^\circ$  but differs less in comparison with the pincer complex 3. On top of figure 4 the packing pattern of 4 in the crystal is displayed along [001]. Two classical hydrogen bonds (details see table 4) between the molecules lead to the formation of a 1D chain that extends in the [111] direction. In a head-to-tail fashion neighboring complex molecules are connected via the ethylester group of the equatorial ligand and the hydroxyl group of the axially coordinating ethanol molecule. The chains are arranged parallelly leading to a layered structure.

For the complexes 1 and 2 it was not possible to obtain single crystals suitable for x-ray structure analysis. Consequently,

**Table 2.** Selected bond lengths (Å) and angles (°) within the inner coordination sphere of the iron(II) pincer-complex [FeL1c(bpeb)] (3) and the side product [FeL1b(EtOH)<sub>2</sub>] (4).

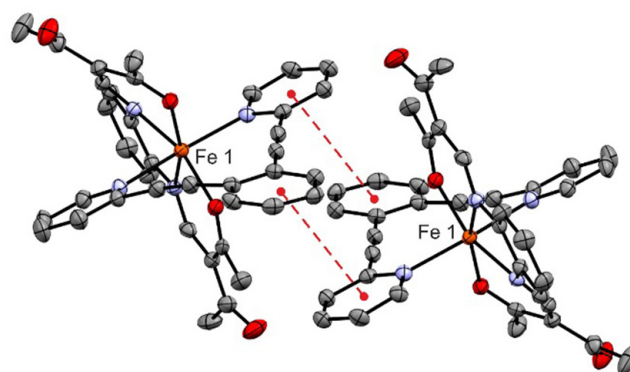
	Fe–N <sub>eq</sub>	Fe–O <sub>eq</sub>	Fe–N/O <sub>ax</sub>	O <sub>eq</sub> –Fe–O <sub>eq</sub>	N/O <sub>ax</sub> –Fe–N/O <sub>ax</sub>
3	2.145(2) 2.127(2)	2.007(2) 2.030(19)	2.221(2) 2.318(2)	116.73(7)	166.89(8)
4	2.1147(11) 2.0917(11)	2.0251(9) 2.0366(9)	2.1997(9) 2.2013(9)	111.73(4)	169.38(4)

**Figure 2.** Molecular packing of the compound 3 in the crystal at 133 K. Top: view along [100] and bottom: view along [010]. Hydrogen atoms have been omitted for clarity. The hydrogen bonds are represented as dashed lines.

the powder x-ray diffraction patterns of those complexes were measured to confirm whether or not the coordination of bpeb was successful. For comparison, the PXRD pattern of the free ligand bpeb was determined as well. The calculated (3 and 4) and measured (1, 2 and bpeb) powder pattern is given in figure 5. The ligand bpeb itself shows a characteristic peak at 22.5° that is absent in the four complexes 1–4. This can be used as indication that no co-precipitation of un-coordinated bpeb and the starting iron complex did occur. This is further supported by a comparison of the PXRD patterns of 2 and 4 that both comprise the same equatorial ligand but show a completely different PXRD pattern. Those considerations in combination with the results from elemental analysis leads to the conclusion that the coordination of bpeb was also successful in 1 and 2.

## 2.2. Magnetic properties

Magnetic susceptibility measurements in the temperature range from 400 K to 50 K were performed to determine the magnetic properties for the three bpeb complexes 1–3, especially with regard to the potential observation of spin crossover. At room temperature, the  $X_M T$  values are as expected for

**Figure 3.** Schematic representation of the  $\pi$ - $\pi$  interactions involved in the packing of 3 in the crystal.

iron(II) high spin complexes: 3.21 cm<sup>3</sup> Kmol<sup>-1</sup> (1), 3.65 cm<sup>3</sup> Kmol<sup>-1</sup> (2) and 3.27 cm<sup>3</sup> Kmol<sup>-1</sup> (3). The room temperature high spin state is confirmed by Mössbauer spectroscopy. For all three complexes only one quadrupole split doublet is observed with quadrupole splitting  $\Delta E_Q \approx 2.25$  mm s<sup>-1</sup> and a conserved isomer shift  $\delta \approx 1.0$  mm s<sup>-1</sup> (summarized in table 5) which both are in the typical range of iron(II) HS complexes of this ligand type [8, 11, 12].

For 2 the full width at half maximum  $\Gamma/2$  is slightly increased compared to 1, since the embedded solvent gives additional degrees of freedom. It therefore increases the full width at half maximum  $\Gamma/2$  due to the lower Lamb-Mössbauer factor ( $F$ ) [24]. In figure 6, the Mössbauer spectrum and the results from the temperature dependent magnetic measurements are given for 1 as typical representative. In the SI, figure S1, the corresponding results for 2 and 3 are given. Upon cooling, the  $X_M T$  product does not change significantly for 1 and 2. The complexes remain in the HS state in the entire temperature range investigated.

## 2.3. Steric effects of the pincer ligand bpeb on SCO

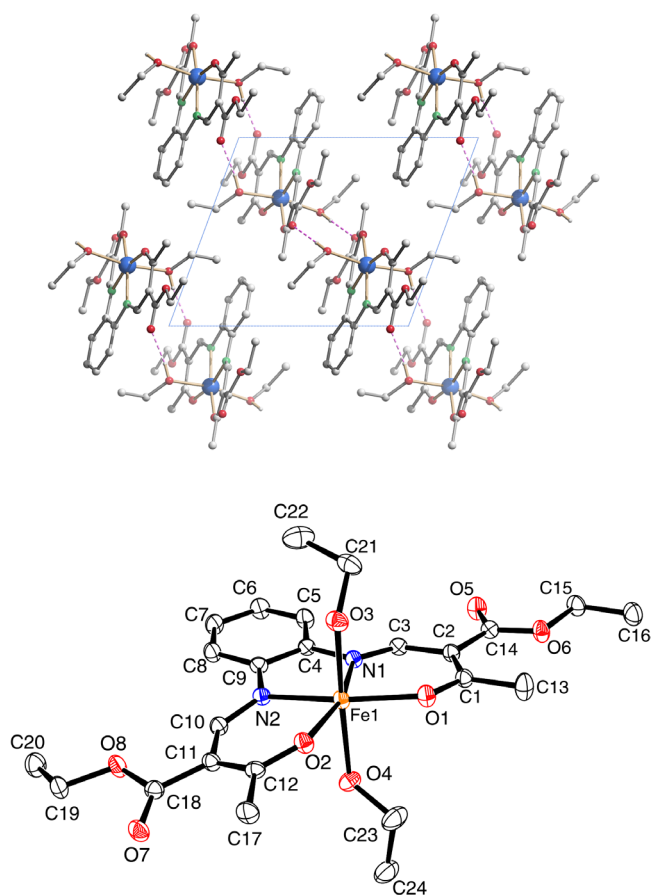
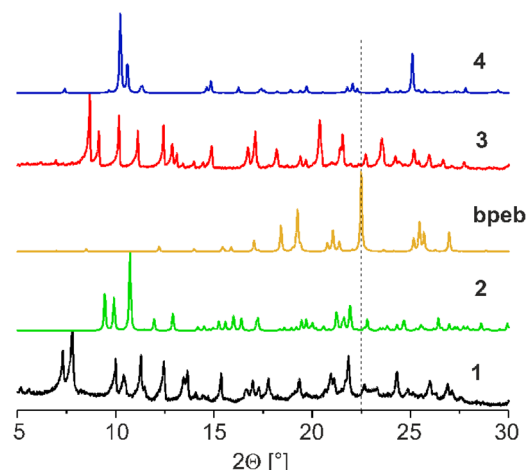
This study took root in the idea that integration of two pyridine donors in a rigid  $\pi$ -planar hydrocarbon backbone, bpeb, which is strongly pre-arranged for *trans*-coordination in an octahedral iron(II) complex will remediate the notorious kinetic lability of the monodentate ligands. The second important idea was that the pincer ligand would not affect significantly the energetics of SCO, due to the unaltered ligand strength. In particular, as previous work generally found the spin state of such complexes to be susceptible to temperature, similar behavior was anticipated for the iron(II) complexes of bpeb reported in this work. Actually, this latter idea proved

**Table 3.** Selected distances (Å) and angles (°) of the  $\pi$ - $\pi$  interaction in **3**. Cg (I) is the centroid of the ring with the number I,  $\alpha$  is the dihedral angle between the rings,  $\beta$  is the angle between the vector Cg (I)  $\rightarrow$  Cg (J) and the normal ring I,  $\gamma$  is the angle between the vector Cg (I)  $\rightarrow$  Cg (J) and the normal ring J.

Cg(I)	Cg(J)	Cg-Cg	$\alpha$	$\beta$	$\gamma$
Cg(1)	Cg(2) <sup>a</sup>	4.047(2)	16.61(13)	24.09	37.14
Cg(1)	Cg(2) <sup>b</sup>	4.002(2)	27.76(13)	31.52	8.99

<sup>a</sup>  $-x, 1-y, -z$ .<sup>b</sup>  $1/2+x, 1/2-y, z$ .**Table 4.** Short contacts observed in the crystal structure of **3** and **4**, with relevant distances (Å) and their angles (°).

	Donor-H...acceptor	D-H	H...A	D...A	D-H...A
<b>3</b>	C(8)-H(8)...O(4) <sup>a</sup>	0.95	2.49	3.278(4)	140
	O(21)-H(21)...O(3) <sup>b</sup>	0.95	2.50	3.418(4)	161
	O(37)-H(37)...O(4) <sup>c</sup>	0.95	2.49	3.383(4)	157
<b>4</b>	O(3)-H(3)...O(7) <sup>d</sup>	0.84	1.89	2.7324(13)	178
	O(4)-H(4)...O(5) <sup>e</sup>	0.84	1.85	2.6797(14)	170

<sup>a</sup>  $1/2+x, 1/2-y, z$ .<sup>b</sup>  $1/2-x, -1/2+y, -z$ .<sup>c</sup>  $x, 1/2+y, 1/2-z$ .<sup>d</sup>  $x, 2-y, 1/2+z$ .<sup>e</sup>  $x, -y, 1-z$ .**Figure 4.** Top: View of the molecular packing along [001]. Hydrogen atoms have been omitted for clarity. The hydrogen bonds are represented as dashed lines. Bottom: ORTEP drawing of the asymmetric unit of **4** with the atom numbering scheme used in the text. Hydrogen atoms are omitted for clarity. Thermal ellipsoids presented at 50% level.**Figure 5.** Powder x-ray diffraction pattern of **1**, **2** and the free ligand bpeb (room temperature), and **3** and **4** (133 K, calculated from single crystal XRD data).**Table 5.** Mössbauer parameters of **1**, **2** and **3** in ( $\text{mm s}^{-1}$ ) at room temperature. All values are given relative to  $\alpha$  iron.

	$\delta$	$\Delta E_Q$	$\Gamma/2$	spin state
<b>1</b>	1.003(7)	2.251(14)	0.145(11)	HS
<b>2</b>	1.009(13)	2.25(3)	0.16(2)	HS
<b>3</b>	1.005(2)	2.27(4)	0.13(3)	HS

wrong in this study. All complexes were found in the HS state, irrespective of temperature state.

Clearly confinement of the two pyridine groups ( $\text{py}$ )<sub>2</sub> within bpeb destabilizes the LS state significantly. The underlying steric reasons of the destabilization have been addressed for complex **3** by DFT modelling methods. Optimization of the HS state of **3** on the BP86/TZVP level of theory (details

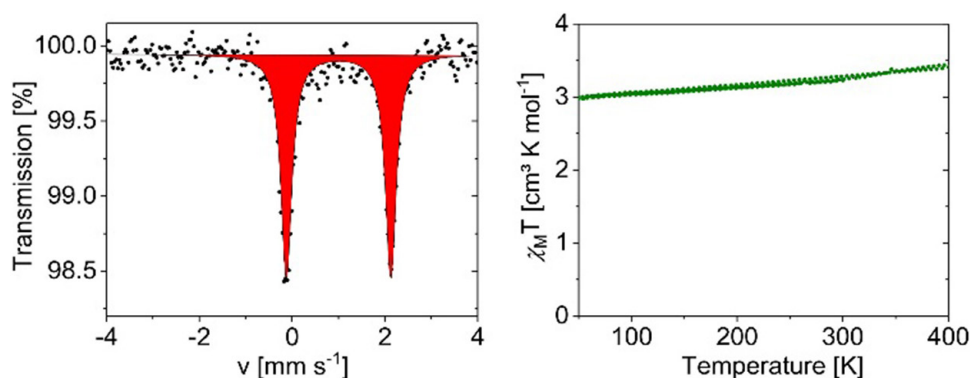


**Figure 6.** Left: Mössbauer spectrum of 1 at room temperature. Right: Plot of the  $\chi_M T$  product versus  $T$  of 1.

in the Experimental Section) fully matched the XRD-derived data (Metrics in table S4, ESI). Accordingly, the DFT-derived structure of elusive LS-3 is regarded as a valid model (Metrics in table S4, ESI). The validity of the chosen method is further corroborated through comparison of the DFT-data of compound  $5^{\text{Me}}$ , lacking the pincer arrangement of  $(\text{py})_2$ , with the close analogue  $5^{\text{Ph}}$ , whose XRD-data have been reported in both spin states (Metrics in table S5, ESI) [33].

Intriguingly, inspection of the assembled structure data of 3 and  $5^{\text{Me/Ph}}$  does not reveal obvious effects of the pincer units on the metrics of the inner coordination sphere. That is, structural divergence, if significant, rather prevails between the accessible HS states of 3 and  $5^{\text{Me/Ph}}$ , whereas the respective LS states are extremely similar.

It should be mentioned here, however, that the reference systems  $5^{\text{Me/Ph}}$  exhibit minimum structures with orthogonally arranged  $\text{py} \perp \text{py}$   $\pi$ -planes, while co-planar  $\text{py} \parallel \text{py}$  is enforced in 3. Indeed, rotated conformers of  $5^{\text{Me}}$  with fixed  $\text{py} \parallel \text{py}$  orientation reside slightly above the ground state in both cases, as revealed by B3LYP\* single-point calculations ( $\Delta E_{\text{conf}} \approx +7 \text{ kJ mol}^{-1}$ ). Nevertheless, pyridine rotation cannot account for the diverging SCO pattern of 3 and 5 as both spin states of 5 are affected in the same direction and to the same extent.

Absolute SCO energies of 3 and  $\text{py} \perp \text{py}$   $5^{\text{Me}}$  obtained with B3LYP\* amount to  $\Delta_{\text{SCO}} E = E(\text{HS}) - E(\text{LS}) = -21.4 \text{ kJ mol}^{-1}$  and  $+14.2 \text{ kJ mol}^{-1}$ , respectively. With a view to the largely conserved inner coordination spheres of 3 and  $5^{\text{Me}}$  the strongly favored HS-configuration in 3 must be associated either or both with steric clash of the pincer backbone and the equatorial ligand L1c and enhanced intraligand strain in the pincer unit. Actually, space-filling models of LS-3 indicate pincer-borne crowding which may reflect in an increase of the equatorial opening O–Fe–O from  $87^\circ$  in undisturbed  $5^{\text{Me}}$  to  $92^\circ$  in 3. Whereas this steric effect is expected to destabilize the LS state in 3, additional results from DFT also regard the spin-state dependent strain in the pincer ligand as a relevant factor. Single-point computation of the bpeb ligand, frozen in the positions of the optimized structures of HS-3 and LS-3, strongly supports the notion of SCO-borne coordination contraction causing significant intraligand strain. The decrease in the non-bonded  $\text{N}_{\text{py}}\text{--}\text{N}_{\text{py}}$  distance from  $4.45 \text{ \AA}$  to  $3.96 \text{ \AA}$  in HS-3 and LS-3, respectively, reflects in a destabilization by

almost  $20 \text{ kJ mol}^{-1}$ . This energy difference is clearly a consequence of intraligand strain, which is absent in the HS- $5^{\text{Me}}$ /LS- $5^{\text{Me}}$  couple with independent monodentate py donors, where an analogous analysis gives almost identical energies ( $\Delta E = 1.4 \text{ kJ mol}^{-1}$ ).

### 3. Conclusion

In this manuscript, the synthesis of three new Schiff base-like pincer complexes is described. The ligand bpeb which pre-arranges two pyridyl donors for axial coordination was used with the aim to increase the stability of iron(II) spin-crossover (SCO) complexes with respect to the known monodentate counterparts. We actually succeeded in the synthesis of three different iron(II) complexes of the pincer ligand presenting the first iron coordination compounds of that ligand type. Intriguingly, different solvents were required for the synthesis depending on the substitution pattern of the respective equatorial ligands. Since the starting material of 3 is hardly soluble in both methanol and ethanol, the synthesis only succeeded in acetonitrile. Otherwise, the bis-solvate complexes  $[\text{FeLx}(\text{MeOH})_2]$  or the corresponding complex  $[\text{FeLx}(\text{EtOH})_2]$  were obtained. The crystal structure of the desired iron(II) pincer complex 3 reveals asymmetric and comparably long bonds between the axial nitrogen atoms of the bpeb and the iron(II) coordination center. This is most likely due to steric hindrance between the triple bond of the pincer ligand and the oxygen donor atoms of the Schiff base-like ligand. This could be a reason why no spin crossover behavior is observed in the magnetic measurement for all three complexes. DFT analysis reveals, in addition, that the strong preference of 3 for the high spin (HS) state can be traced to intraligand strain in the pincer ligand, which raises an energy penalty towards SCO-related contraction. The sum of restraining interactions most probably interferes with the required shortening of the bond lengths during spin crossover. In consequence, 1–3, as studied herein do not undergo SCO, although the pincer ligand itself had been previously shown to support M–N bond lengths in the range of  $1.91\text{--}2.63 \text{ \AA}$  which covers the usual range of iron-dependent SCO. Additional electronic stabilization of the low spin state will be necessary to outweigh the strain induced preference for the HS state.

## 4. Experimental section

**[FeL1a(bpeb)]** (1) A solution of [FeL1a(MeOH)<sub>2</sub>] (0.20 g, 0.42 mmol) and bpeb (0.24 g, 0.86 mmol) in methanol (5 ml) was heated to reflux for 2 h. After cooling and left to stand at room temperature for 24 h, the precipitated brown powder was filtered off, washed with methanol (2 × 2 ml) and dried in vacuo to give 1 (yield 0.13 g, 45%). **IR:**  $\tilde{\nu}$  = 2222 (m,  $\nu$ [C≡C]), 1771 (m,  $\nu$ [C=O]), 1677 & 1561 (s,  $\nu$ [C=N]), 1489 & 1400 (vs,  $\nu$ [C=C<sub>Ar</sub>]), 1261 (vs,  $\nu$ [C-O]), 1194 (s,  $\nu$ [C-N]). **-MS** (DEI(+), 70 eV): m/z (%): 428 (100) [M-C<sub>19</sub>H<sub>11</sub>N<sub>2</sub><sup>3+</sup>], 382 (45) [C<sub>17</sub>H<sub>14</sub>FeN<sub>2</sub>O<sub>5</sub>], 340 (55) [C<sub>15</sub>H<sub>12</sub>FeN<sub>2</sub>O<sub>4</sub><sup>2+</sup>], 309 (78) [C<sub>14</sub>H<sub>9</sub>FeN<sub>2</sub>O<sub>3</sub><sup>3+</sup>], 280 (47) [bpeb<sup>+</sup>]. Elemental analysis calcd (%) for C<sub>38</sub>H<sub>30</sub>FeN<sub>4</sub>O<sub>6</sub> (694.53 g mol<sup>-1</sup>): C 65.72; H 4.35; N 8.07; found: C 65.49; H 4.62; N 7.86.

**[FeL1b(bpeb)] · (EtOH)** (2) A solution of [FeL1b(MeOH)<sub>2</sub>] (0.15 g, 0.30 mmol) and bpeb (0.17 g, 0.60 mmol) in ethanol (10 ml) was heated to reflux for 2 h. After cooling and left to stand at -18 °C for 24 h, the precipitated red to brown powder was filtered off, washed with ethanol (2 × 2 ml) and dried in vacuo to give 2 (yield 0.11 g, 48%). **IR:**  $\tilde{\nu}$  = 2216 (m,  $\nu$ [C≡C]), 1684 & 1549 (s,  $\nu$ [C=N]), 1566 & 1489 (vs,  $\nu$ [C=C<sub>Ar</sub>]), 1261 (vs,  $\nu$ [C-O]), 1194 (s,  $\nu$ [C-N]). **-MS** (DEI(+), 70 eV): m/z (%): 442 (26) [C<sub>20</sub>H<sub>22</sub>FeN<sub>2</sub>O<sub>6</sub><sup>+</sup>], 397 (22) [C<sub>18</sub>H<sub>17</sub>FeN<sub>2</sub>O<sub>5</sub>], 340 (55) [C<sub>15</sub>H<sub>12</sub>FeN<sub>2</sub>O<sub>4</sub><sup>2+</sup>], 354 (39) [C<sub>16</sub>H<sub>14</sub>FeN<sub>2</sub>O<sub>4</sub><sup>2+</sup>], 309 (29) [C<sub>14</sub>H<sub>9</sub>FeN<sub>2</sub>O<sub>3</sub><sup>3+</sup>], 280 (62) [bpeb<sup>+</sup>]. Elemental analysis calcd (%) for C<sub>42</sub>H<sub>40</sub>FeN<sub>4</sub>O<sub>7</sub> (768.65 g mol<sup>-1</sup>): C 65.63; H 5.25; N 7.29; found: C 65.55; H 5.29; N 7.66.

**[FeL1c(bpeb)]** (3) A solution of [FeL1c(MeOH)<sub>2</sub>] (0.16 g, 0.36 mmol) and bpeb (0.20 g, 0.71 mmol) in acetonitrile (10 ml) was heated to reflux for 2.5 h. After cooling and left to stand at room temperature for two weeks, the precipitated black crystalline solid was filtered off, washed with acetonitrile (1 × 1 ml) and dried in vacuo to give 3 (yield 0.14 g, 59 %). **IR:**  $\tilde{\nu}$  = 2211 (w,  $\nu$ [C≡C]), 1633 & 1561 (s,  $\nu$ [C=N]), 1261 (vs,  $\nu$ [C-O]), 1200 (s,  $\nu$ [C-N]). **-MS** (DEI(+), 70 eV): m/z (%): 382 (100) [C<sub>18</sub>H<sub>18</sub>FeN<sub>2</sub>O<sub>4</sub><sup>2+</sup>], 257 (69) [C<sub>12</sub>H<sub>11</sub>FeNO<sub>2</sub><sup>5+</sup>], 176 (10) [C<sub>10</sub>H<sub>10</sub>NO<sub>2</sub><sup>3+</sup>]. Elemental analysis calcd (%) for C<sub>38</sub>H<sub>30</sub>FeN<sub>4</sub>O<sub>4</sub> (662.51 g mol<sup>-1</sup>): C 68.89; H 4.56; N 8.46; found: C 68.64; H 4.59; N 8.45.

### 4.1. Computation details

The molecular structures of compound 3 and model complex 5<sup>Me</sup> lacking the chelate pincer ([FeL1c(py)<sub>2</sub>]) were optimized in their singlet and quintet spin states in ORCA [27] with the BP86 functional [28] and basis sets of triple- $\zeta$  quality.[29] Model complex 5 was additionally optimized with the orientation of axial pyridines fixed to co-planar, in order to mimic the (py)<sub>2</sub> arrangement in 3. Electronic energies were obtained from single-point calculations with the hybrid functional B3LYP\*, with exact exchange  $a_0 = 0.15$  empirically parameterized to match S CO energies.[30] Solvent effects were approximated within the COSMO approach parameterized for MeCN.[31] Dispersion was treated with Grimme's D3 approach.[32] Structure plots and tabulated structural metrics

are compiled in the Supporting Information (figures S2–S5 and tables S4 and S5).

## Acknowledgments

Financial support from the German Science Foundation (SFB840) and the University of Bayreuth is gratefully acknowledged.

## ORCID iDs

Gerald Hörner  <https://orcid.org/0000-0002-3883-2879>

Birgit Weber  <https://orcid.org/0000-0002-9861-9447>

## References

- [1] Halcrow M A (ed) 2013 *Spin-Crossover Materials* (Chichester: Wiley)
- [2] Gütlich P and Goodwin H A (ed) 2004 *Spin Crossover in Transition Metal Compounds I-III* (Berlin: Springer)
- [2] Meded V, Bagrets A, Fink K, Chandrasekar R, Ruben M, Evers F, Bernand-Mantel A, Seldenthuis J S, Beukman A and van der Zant H S J 2011 *Phys. Rev. B* **83** 2327
- Miyamachi T et al 2012 *Nat. Commun.* **3** 938
- Gopakumar T G, Matino F, Naggert H, Bannwarth A, Tuzek F and Berndt R 2012 *Angew. Chem., Int. Ed.* **51** 6262–6
- Burzuri E, García-Fuente A, García-Suárez V, Senthil Kumar K, Ruben M, Ferrer J and van der Zant H S J 2018 *Nanoscale* **10** 7905–11
- Aravena D and Ruiz E 2012 *J. Am. Chem. Soc.* **134** 777–9
- [3] Tissot A, Bardeau J-F, Rivière E, Brisset F and Boillot M-L 2010 *Dalton Trans.* **39** 7806
- Tissot A, Rechignat L, Bousseksou A and Boillot M-L 2012 *J. Mater. Chem.* **22** 3411
- Shi S et al 2009 *Appl. Phys. Lett.* **95** 43303
- Gopakumar T G et al 2013 *Chem. Eur. J.* **19** 15702–9
- Davesne V et al 2015 *J. Chem. Phys.* **142** 194702
- [4] Boillot M-L and Weber B 2018 *C. R. Chim.* **21** 1196–208
- [5] Weber B, Bauer W, Pfaffeneder T, Dürst M M, Naik A D, Rotaru A and Garcia Y 2011 *Eur. J. Inorg. Chem.* **21** 3193–206
- Bauer W, Ossiander T and Weber B 2018 *Frontiers Chem. Sci. Eng.* **12** 400–8
- [6] Bauer W, Ossiander T and Weber B 2010 *Z. Naturforsch. B* **65b** 323–8
- [7] Weber B 2009 *Coord. Chem. Rev.* **253** 2432–49
- [8] Weber B and Jäger E-G 2009 *Eur. J. Inorg. Chem.* **4** 465–77
- [9] Lochenie C, Schötz K, Panzer F, Kurz H, Maier B, Puchtlar F, Agarwal S, Köhler A and Weber B 2018 *J. Am. Chem. Soc.* **140** 700–9
- [10] Weber B, Kaps E and Dankhoff K 2017 *Z. Anorg. Allg. Chem.* **643** 1593–9
- Weber B, Obel J, Lorenz L R, Bauer W, Carrella L and Rentschler E 2009 *Eur. J. Inorg. Chem.* **36** 5535–40
- [11] Weihermüller J et al 2019 *J. Mater. Chem. C* **7** 1151–63
- [12] Weihermüller J, Schlamp S, Dittrich B and Weber B 2019 *Inorg. Chem.* **58** 1278–89
- [13] Weber B, Obel J, Henner-Vasquez D and Bauer W 2009 *Eur. J. Inorg. Chem.* **36** 5527–34
- Weber B, Bauer W and Obel J 2008 *Angew. Chem., Int. Ed.* **47** 10098–101

- [14] Phonsri W, Davies C G, Jameson G N L, Moubaraki B and Murray K S 2016 *Chem.-Eur. J.* **22** 1322–33  
Phonsri W, Martinez V, Davies C G, Jameson G N L, Moubaraki B and Murray K S 2016 *Chem. Commun.* **52** 1443–6  
Phonsri W, Macedo D S, Davies C G, Jameson G N L, Moubaraki B and Murray K S 2017 *Dalton Trans.* **46** 7020–9  
Phan H V et al 2012 *Chem. Eur. J.* **18** 15805–15  
Barrios L A, Bartual-Murgui C, Peyrecave-Lleixa E, Le Guennic B, Teat S J, Roubeau O and Aromi G 2016 *Inorg. Chem.* **55** 4110–6  
Costa J S, Rodríguez-Jiménez S, Craig G A, Barth B, Beavers C M, Teat S J and Aromí G 2014 *J. Am. Chem. Soc.* **136** 3869–74
- [15] Selander N and Szabó K J 2011 *Chem. Rev.* **111** 2048–76  
[16] Bosch E and Barnes C L 2001 *Inorg. Chem.* **40** 3097–100  
[17] Hu Y-Z, Chamchoumis C, Grebowicz J S and Thummel R P 2002 *Inorg. Chem.* **41** 2296–300  
[18] Fiscus J E, Shotwell S, Layland R C, Smith M D, Zur Loye H-C and Bunz U H F 2001 *Chem. Commun.* **24** 2674–5  
[19] Barnes C L and Bosch E 2006 *J. Chem. Crystallogr.* **36** 563–6  
[20] Jäger E-G, Häussler E, Rudolph M and Schneider A 1985 *Z. Anorg. Allg. Chem.* **525** 67–85  
[21] Schlamp S, Thoma P and Weber B 2014 *Chem. Eur. J.* **20** 6462–73  
[22] Weber B and Jäger E-G 2009 *Z. Anorg. Allg. Chem.* **635** 130–3
- [23] Weber B and Kaps E 2005 *Heteroatom Chem.* **16** 391–7  
[24] Gütlich P, Bill E and Trautwein A X 2011 *Mössbauer Spectroscopy and Transition Metal Chemistry* (Springer, Berlin, Heidelberg)  
[25] Guionneau P, Marchivie M, Bravic G, Létard J-F and Chasseau D 2004 Structural Aspects of Spin Crossover. Example of the  $[\text{Fe}^{\text{II}}\text{L}_n(\text{NCS})_2]$  Complexes. In: Spin Crossover in Transition Metal Compounds II. *Top. Curr. Chem.* (Springer, Berlin, Heidelberg) **234** 97–128  
[26] Weber B, Kaps E, Weigand J, Carbonera C, Létard J-F, Achterhold K and Parak F G 2008 *Inorg. Chem.* **47** 487–96  
[27] Neese F 2012 *WIREs Comput. Mol. Sci.* **2** 73–8  
[28] Becke A D 1988 *Phys. Rev. A* **38** 3098–100  
[29] Schäfer A, Horn H and Ahlrichs R 1992 *J. Chem. Phys.* **97** 2571–7  
[30] Becke A D 1993 *J. Chem. Phys.* **98** 5648–52  
Lee C, Yang W and Parr R G 1988 *Phys. Rev. B* **37** 785–9  
Reiher M, Salomon O and Hess B A 2001 *Theor. Chem. Acc.* **107** 48–55  
[31] Grimme S, Antony J, Ehrlich S and Krieg H 2010 *J. Chem. Phys.* **132** 154104  
[32] Klamt A and Schüürmann G 1993 *J. Chem. Soc. Perkin Trans. 2* **5** 799–805  
[33] Lochenie C, Heinz J, Milius W and Weber B 2015 *Dalton Trans.* **44** 18065–77